Memristor-Coupled Logistic Hyperchaotic Map

Bocheng Bao, *Member, IEEE*, Kang Rong, Houzhen Li, *Graduate Student Member, IEEE*, Kexin Li, Zhongyun Hua, *Member, IEEE*, and Xi Zhang, *Member, IEEE*

Abstract—The continuous memristor models have been applied to various chaotic circuits. However, the discrete memristor models and their applications to discrete maps haven't attracted much attention, yet. In this brief, we first present a discrete memristor model and analyze its characteristics. By coupling the model into the Logistic map, a memristive Logistic map is further achieved. Due to the existence of line fixed point, the memristive Logistic map can be unstable or critically stable, depending on its control parameters and initial state. Using several analysis methods, we study the control parameters-relied dynamical behaviors of the memristive Logistic map and disclose its hyperchaotic attractors. The numerical results show that the discrete memristor can efficiently improve the chaos complexity in the Logistic map. In addition, digital experiments are designed to validate the numerical results.

Index Terms—Digital experiment, discrete memristor, fixed point, hyperchaos, memristive logistic map.

I. Introduction

CHAOTIC behaviors can be displayed by continuous oscillation systems or discrete iterative maps [1]–[3]. To achieve chaotic oscillations, a dynamical system must have one or more nonlinear terms, which include the polynomial, absolute value, trigonometric, and exponential terms and so on. Thus, the nonlinear terms play a significant role in generating chaotic oscillations. However, these nonlinear terms usually involved in chaotic oscillations do not contain any inner states. As a fundamental circuit element [4], the memristor owns a special nonlinearity and its nonlinear memristance or memductance is controlled by the electric charge or magnetic flux [5]. With an inner state, the memristor is entirely different from the traditional nonlinear elements and it can be used to construct numerous oscillating circuits for achieving complex chaotic oscillations [6].

A hyperchaotic system has at least two positive Lyapunov exponents, while a normal chaotic system has only one. Thus, the hyperchaos usually has more complex dynamics than the normal chaos and it is more applicable for many

chaos-based security applications [7]. To achieve the hyperchaotic behavior, a continuous system should have more than four dimensions, while a discrete map needs only two dimensions [8]. Thus, compared with the continuous system, the discrete map has simpler algebraic structure [9] and higher calculation efficiency. This is suitable for many applications with limited resources [7], [10]. Except for several specially designed two-dimensional (2D) discrete maps [9], [11], however, most 2D discrete maps cannot achieve hyperchaotic oscillations [12], [13]. In brief, generating hyperchaos in a 2D discrete map with simple algebraic structure is an interesting and meaningful research topic in the field of chaos theory and its application [14].

Recently, a discrete memristor with cosine memductance was derived from a continuous memristor using a forward Euler difference algorithm [9]. Then, several 2D memristive discrete maps were presented through introducing the discrete memristor into some well-known one-dimensional (1D) discrete maps [15]. Because the cosine memductance designed in [15] are bounded above and below, the discrete memristor can be easily coupled into existing discrete maps. Different from the discrete memristor with cosine memductance, this brief presents a charge-controlled discrete memristor model with quadratic memristance. It is similar with the continuous flux-controlled memristor owning quadratic memductance in [16]. By coupling the presented discrete memristor into the 1D Logistic map [17], a 2D memristor-coupled Logistic map with a line fixed point is then achieved. Numerical analyses and experimental results show that the 2D memristive map is hyperchaotic. Thus, it is an effective method to enhance the chaos complexity of the Logistic map by coupling a discrete memristor into the map.

II. Memristor Discrete Model

This section first presents a discrete memristor model with quadratic memristance using a forward Euler difference algorithm, and then demonstrates its characteristics.

Presented by Professor Chua in [18], the continuous memristor model with quadratic memristance is written as

$$v(t) = M(q)i(t) = [a + bq^2(t)]i(t),$$
$$dq(t)/dt = i(t), \tag{1}$$

where $i(t)$ and $v(t)$ represent the input current and output voltage, respectively, $q(t)$ denotes the inner charge while $M(q) = a + bq^2(t)$ is the quadratic memristance with two inner control parameters a and b. Similar to the continuous memristor owning quadratic memductance reported in [16],
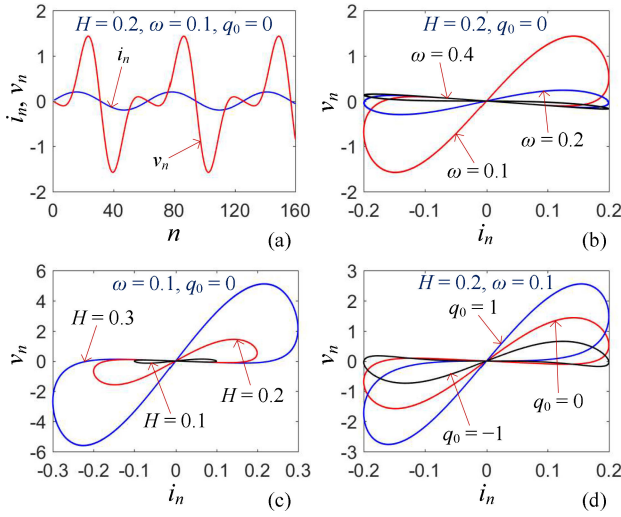
Fig. 1. Characteristics of the discrete memristor when being applied to a discrete sinusoidal current $i_n = H \sin(\omega n)$, where $a = -1$ and $b = 1$. (a) Current and voltage sequences. (b) Frequency-depended loci. (c) Amplitude-depended loci. (d) Initial state-depended loci.

the continuous memristor described in (1) can also show a distinct hysteresis loop pinched at the origin when being applied a continuous sinusoidal current.

Assume that i_n, v_n, and q_n stand for the sampling points of $i(t)$, $v(t)$, and $q(t)$ at the unit time n, respectively. Using the same strategy for discretizing a continuous memristor model [7], a discrete memristor model can be yielded by discretizing the charge-controlled memristor described in (1) using the forward Euler difference algorithm as

$$v_n = M(q_n)i_n = (a + bq_n^2)i_n,$$
$$q_{n+1} = q_n + \Delta T \cdot i_n, \tag{2}$$

where q_{n+1} represents the sampling point of $q(t)$ at the unit time $(n + 1)$ and ΔT indicates the step size in each unit time. Generally, set $\Delta T = 1$. The discrete model in (2) can also be considered as a discrete memristor. Obviously, this discrete memristor owns a special nonlinearity with an inner state q_n.

To quantitatively show the characteristics of the discrete memristor, a discrete sinusoidal current $i_n = H \sin(\omega n)$ is added to the memristor. Denote the inner control parameters of the discrete memristor as $a = -1$ and $b = 1$. For $H = 0.2$, $\omega = 0.1$, and $q_0 = 0$, Fig. 1(a) depicts the input i_n and the related output v_n with respect to the iteration number. For $\omega = 0.1$, 0.2, and 0.4 with $H = 0.2$ and $q_0 = 0$, the frequency-depended loci in the $i_n - v_n$ plane are plotted in Fig. 1(b). For $H = 0.1$, 0.2, and 0.3 with $\omega = 0.1$ and $q_0 = 0$, the amplitude-depended loci in the $i_n - v_n$ plane are given in Fig. 1(c). Moreover, for $q_0 = 1$, 0, and -1 with $H = 0.2$ and $\omega = 0.1$, the initial state-depended loci in the $i_n - v_n$ plane are illustrated in Fig. 1(d). The numerical results in Fig. 1(b)-(d) can perfectly display the elegant hysteresis loops pinched at the origin [18].

In addition, the initial state-depended loci also prove that the discrete memristor can embody the memory effect. The change of the initial state will cause the difference of the local active property, which can result in complex dynamics when the discrete memristor is coupled into discrete maps.

III. MEMRISTOR-COUPLED LOGISTIC MAP

The well-known Logistic map is a 1D discrete map with one control parameter [17]. It has simple algebraic structure. With the fast development of artificial intelligence (AI), researchers found that the short-term behaviors of some chaotic behaviors can be estimated using AI if the chaotic oscillation has a simple algebraic structure [19]. For example, the short-term behaviors of the Logistic map can be predicated using multilayer perceptions and partially recurrent nets [20].

To improve the chaos complexity of the Logistic map, a memristor-coupled Logistic map, also called memristive Logistic map for short, is presented by coupling the discrete memristor described in (2) into the Logistic map. Thus, the memristive Logistic map can be modeled as

$$x_{n+1} = \mu(1 - x_n)x_n + k(a + bq_n^2)x_n,$$
$$q_{n+1} = q_n + x_n, \tag{3}$$

in which x_n and μ represent the input and control parameter of the Logistic map, respectively, and k stands for the coupling parameter between the discrete memristor and Logistic map.

Because of the involvement of the discrete memristor, the memristive Logistic map has two dimensions and its algebraic structure becomes more complex, which results in the appearance of complex dynamics herein.

The fixed point theory can be used to analyze the stability of a discrete map. The fixed point $(\tilde{x}, \tilde{q})$ of the memristive Logistic map can be solved from the following equations

$$\tilde{x} = \mu(1 - \tilde{x})\tilde{x} + k(a + b\tilde{q}^2)\tilde{x},$$
$$\tilde{q} = \tilde{q} + \tilde{x}, \tag{4}$$

Obviously, the memristive Logistic map has a line fixed point and the line fixed point is demonstrated as

$$S = (\tilde{x}, \tilde{q}) = (0, \eta), \tag{5}$$

where η is an arbitrary constant, determining by the initial position of the inner state q. Accordingly, the Jacobian matrix of the memristive Logistic map at S is given by

$$\mathbf{J} = \begin{bmatrix} \mu + k(a + b\eta^2) & 0 \\ 1 & 1 \end{bmatrix}. \tag{6}$$

And its characteristic polynomial can be obtained as

$$P(\lambda) = (\lambda - 1)[\lambda - \mu - k(a + b\eta^2)], \tag{7}$$

Therefore, two eigenvalues λ_1 and λ_2 can be calculated as

$$\lambda_1 = 1, \quad \lambda_2 = \mu + k(a + b\eta^2). \tag{8}$$

If $|\lambda_1| < 1$ and $|\lambda_2| < 1$, the line fixed point S is stable; otherwise it is unstable. As can be observed from (8), $\lambda_1 = 1$, while λ_2 is depended on the control parameters μ and k as well as the initial state η and inner control parameters a and b of the discrete memristor. Consequently, the line fixed point of the memristive Logistic map can be unstable or critically stable.

When $a = -1$ and $b = 1$ are employed, the critically stable region of the initial state η can be calculated from (8) as

$$\sqrt{k - (\mu + 1)/k} < |\eta| < \sqrt{k - (\mu - 1)/k}. \tag{9}$$

If the initial state η falls into the above region, the memristive Logistic map asymptotically tends to a stable point; otherwise
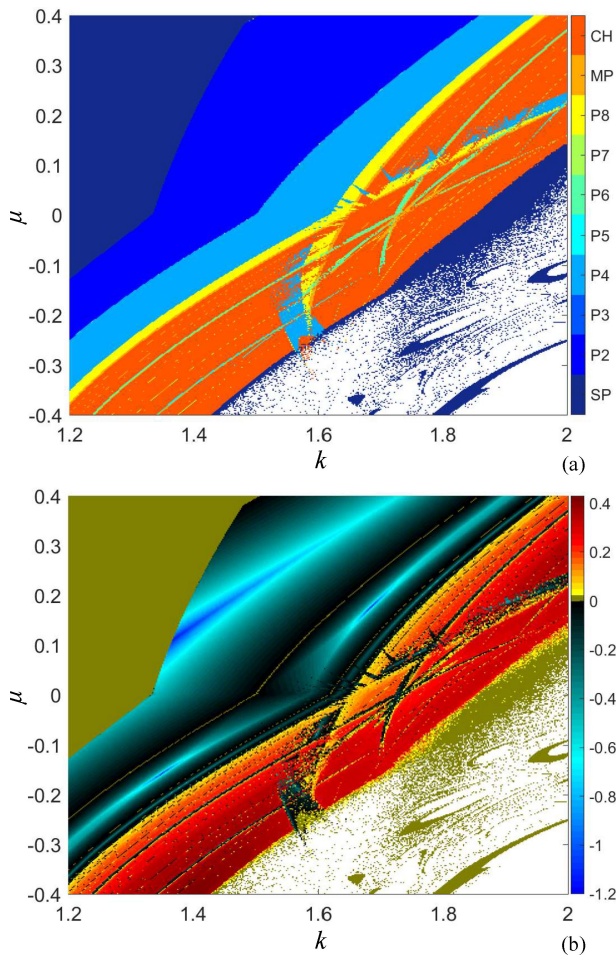
Fig. 2. For fixed $a = -1$, $b = 1$, and $(x_0, q_0) = (0.5, 0.5)$, complex dynamical behaviors of the memristive Logistic map in the $k - \mu$ parameter plane. (a) 2D bifurcation plot according to the cycle number of iterative sequences. (b) 2D dynamical map by computing the LLE of iterative sequences.

it generates either a limit cycle or a chaotic attractor. Thus, the phenomenon of coexisting attractor with bi-stability can occur in the memristive Logistic map.

IV. HYPERCHAOS IN MEMRISTIVE LOGISTIC MAP

To exhibit the dynamics of the memristive Logistic map, we study its control parameters-relied dynamical behaviors in terms of the bifurcation plot, dynamical map, and phase plane plot. The inner parameters of the discrete memristor are set as $a = -1$, $b = 1$, and the initial states of the memristive Logistic map are fixed as $(x_0, q_0) = (0.5, 0.5)$.

A. Two-Dimensional Parameters-Relied Dynamics

A bifurcation plot is drawn in the 2D parameter plane by detecting the cycle number of a discrete map's iterative sequences [21]. Fig. 2(a) paints the bifurcation plot of the memristive Logistic map for $k \in [1.2, 2]$ and $\mu \in [-0.4, 0.4]$. The parameter areas are painted using different colors according to the cycle number of iterative sequences. Specifically, the white denotes the unbounded behavior, the red labeled by CH denotes the chaos, the orange labeled by MP denotes the multi-period, the dark-blue labeled by SP denotes the stable point, and the other colors labeled by P2, P3, to P8 denote period-2,
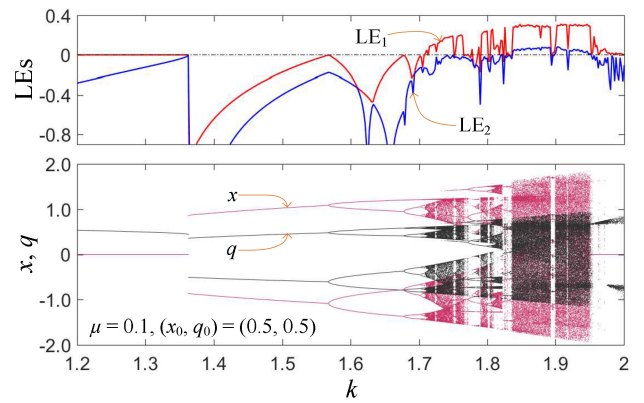

Fig. 3. For fixed $a = -1$, $b = 1$, $\mu = 0.1$, and $(x_0, q_0) = (0.5, 0.5)$, the bifurcation plots of the output x and q (bottom) and the corresponding LEs (top) with the increment of the coupling parameter k.

period-3, to period-8, respectively. It is easily observed that the painted colors change from blue (period-2), to cornflower blue (period-4), further to yellow (period-8), and ultimately to red (chaos), implying the occurrence of the period-doubling bifurcation. Besides, the periodic windows for period-4 and period-7 can be observed in the parameter plane.

A dynamical map can be depicted in the 2D parameter plane by computing its largest Lyapunov exponents (LLEs) [22]. Fig. 2(b) describes the LLEs of the memristive Logistic map under the same parameter areas of the 2D bifurcation plot in Fig. 2(a) and different LLEs are painted as different colors. The positive LLE areas are marked as the yellow-red-brown and a positive LLE denotes chaos, the zero LLE areas are marked as the dark-yellow and a zero LLE denotes stable point, and the negative LLE areas are marked as the black-cyan-blue and a negative LLE denotes period. Hence, the dynamical map in Fig. 2(b) can also be used to characterize the dynamical behaviors of the memristive Logistic map and it is an effective supplementary of the bifurcation plot in Fig. 2(a). Note that the areas marked as white represent the unbounded behavior.

In brief, the memristive Logistic map can show complex dynamical behaviors that are completely depended on the coupling parameter k and control parameter μ.

B. Bifurcation Behaviors and Hyperchaotic Attractors

When exploring the bifurcation behaviors of the memristive Logistic map, we preset the control parameter $\mu = 0.1$ and the coupling parameter k as a variable parameter. Fig. 3 displays its bifurcation plots and Lyapunov exponents (LEs) with the increment of k. Here, the Wolf's Jacobian algorithm is used to calculate the LEs. As shown in Fig. 3, the memristive Logistic map exhibits hyperchaotic behavior in a relatively wide parameter region and displays complex dynamics including stable point, period, chaos, hyperchaos, and periodic windows. In addition, with the increment of k, the memristive Logistic map has a period-doubling bifurcation route.

Two groups of parameter settings are chosen from different color areas in Fig. 2. The phase plane plots of the memristive Logistic map under these parameter settings are numerically simulated and displayed in Fig. 4. Observed from Fig. 4, two types of hyperchaotic attractors and their iterative sequences
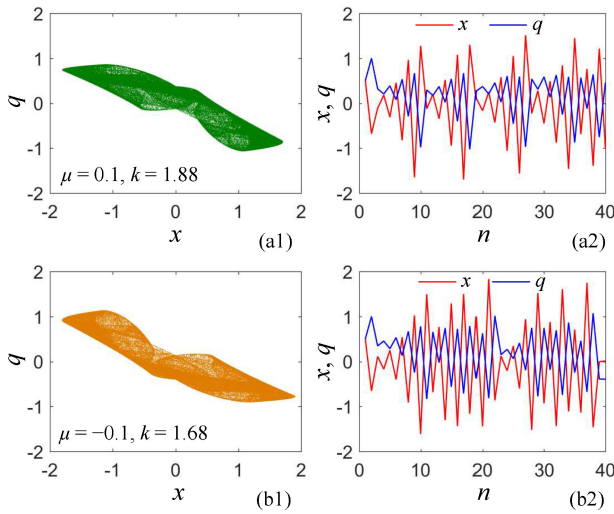
Fig. 4. For two typical groups of parameter settings, the phase plane plots and iterative sequences of the hyperchaotic attractors of the memristive Logistic map. (a1) Phase plane plot and (a2) iterative sequences for $\mu = 0.1$, $k = 1.88$. (b1) Phase plane plot and (b2) iterative sequences for $\mu = -0.1$, $k = 1.68$.

Fig. 5. The bi-stability phenomena in the memristive Logistic map for two groups of parameter settings. (a) For $\mu = 0.1$, $k = 1.88$, the basin of attraction (a1) and coexisting attractors (a2). (b) For $\mu = -0.1$, $k = 1.68$, the basin of attraction (b1) and coexisting attractors (b2).

TABLE I
PERFORMANCE FOR HYPERCHAOTIC ATTRACTORS GIVEN IN FIG. 4

Parameter settings	LE_1, LE_2	SE	PE	CorDim
$\mu = 0.1$, $k = 1.88$	0.2896, 0.0666	0.7877	3.5772	1.5252
$\mu = -0.1$, $k = 1.68$	0.2859, 0.0754	0.7981	3.6031	1.5277

are obtained. Obviously, the iterative sequences have irregular motions.

Besides, we also evaluate the performance indicators of two hyperchaotic attractors generated by the memristive Logistic map in Fig. 4. These performance indicators mainly include the LEs (LE_1, LE_2), spectral entropy (SE) [22], permutation entropy (PE) [23], and correlation dimension (CorDim) [24]. The length of the used hyperchaotic sequences is 10^5 and Table I lists the calculation results of the performance indicators. It shows that the hyperchaotic attractors have good performance indicators, which means that the memristive Logistic map is suitable for many chaos-based security applications. This implies that the introduced discrete memristor can improve the chaos complexity of the Logistic map.

C. Attraction Basins and Coexisting Attractors

To measure the bi-stable behaviors of the memristive Logistic map, the basin of attraction is employed to classify the initial state regions following different oscillation behaviors [25]. For two typical groups of parameter settings, the basins of attraction are colorfully labeled by detecting every initial state in the $x_0 - q_0$ plane and drawn in Fig. 5(a1) and (b1). The cyan, blue, and white areas represent the initial state regions that can trigger the hyperchaotic attractor (HCA), stable point attractor (SPA) and unbounded behavior, respectively. Thus, the memristive Logistic map is bi-stable and can generate coexisting hyperchaotic and point attractors.

According to the critically stable region shown in (9), the line fixed point of the memristive Logistic map with the given parameter settings can be unstable or critically stable
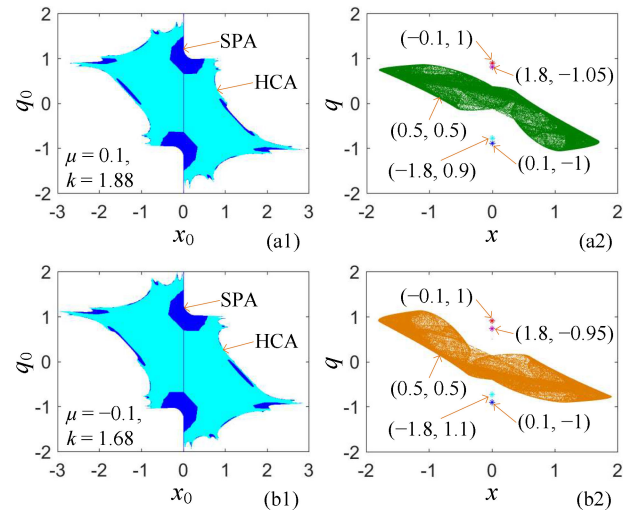
at different memristor initial states. When the memristor initial state is within the critically stable region, the memristive Logistic map may also generate a SPA that is coexisted with a HCA. This indicates that the memristive Logistic map can emerge the bi-stability phenomenon of coexisting hyperchaotic and point attractors.

Besides, Fig. 5(a2) and (b2) demonstrate the phase plane plots of coexisting hyperchaotic and point attractors for two typical groups of parameter settings. The hyperchaotic attractor in Fig. 5(a2) begins with the initial state within the whole cyan region of Fig. 5(a1); whereas the four point attractors in Fig. 5(a2) with different positions separately starts from four initial states within four disconnected blue regions in Fig. 5(a1). Similarly, the coexisting hyperchaotic and point attractors in Fig. 5(b2) start from different attraction regions in Fig. 5(b1). The results in Fig. 5(a) and (b) verify the emergences of bi-stability in the memristive Logistic map.

V. VALIDATION BY DIGITAL EXPERIMENTS

Since the memristive Logistic map is a discrete dynamical system, it is more convenient and simpler to implement it in a digital hardware platform than in an analog hardware platform. So to validate the numerical results of the memristive Logistic map, we design digital experiments on a hardware platform. The hardware platform consists of one 32-bit STM32F407 microcontroller, two 12-bit TLV5618 D/A converters, and some peripherally-linked circuits. According to the discrete memristor model in (2) and memristive Logistic map in (3), we first code their expressions to be executable programs using C language and then load the programs to the microcontroller. All the control parameters and initial states are preloaded to the hardware platform. When turning on the power supply, the voltage signals can be displayed by a digital oscilloscope.

Following the results in Fig. 1, the characteristics of the discrete memristor are experimentally captured in Fig. 6. Similarly, according to the results in Fig. 4(a2) and (b2), the hyperchaotic voltage sequences for two groups of control parameter settings are displayed in Fig. 7. The digital
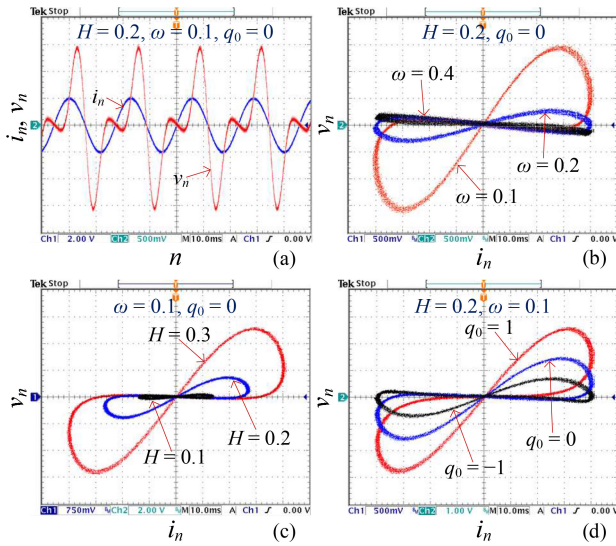
Fig. 6. The experimentally captured characteristics of the discrete memristor. (a) Current and voltage sequences. (b) Frequency-depended loci. (c) Amplitude- depended loci. (d) Initial state-dependent loci.
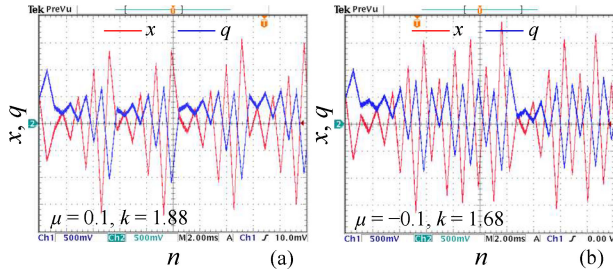

Fig. 7. The experimentally displayed hyperchaotic voltage sequences of the memristive Logistic map for two typical groups of parameter settings. (a) $\mu = 0.1$, $k = 1.88$. (b) $\mu = -0.1$, $k = 1.68$.

experiments perfectly validate the numerical results, which manifest the feasibility of the hardware platform for the presented discrete memristor and memristive Logistic map.

VI. CONCLUSION

Because of the special nonlinearity, a memristor can induce complex dynamical behaviors to an oscillation circuit. To investigate the memristor effect in improving the complexity of discrete map, this brief first constructed a discrete memristor model and then achieved a 2D memristive map by coupling the model into the Logistic map. The unique characteristics of the discrete memristor were quantitatively demonstrated and the stability of the 2D memristive Logistic map was theoretically analyzed. The study results proved the effect of the discrete memristor in improving the chaos complexity and showed that the 2D memristive Logistic map can produce hyperchaotic attractors with excellent performance indicators. Besides, digital experiments were performed to validate the numerical results. With complex dynamics, the applications of the achieved memristive Logistic map are worth investigating.

REFERENCES

[1] M. Chen, M. Sun, H. Bao, Y. Hu, and B. Bao, "Flux-charge analysis of two-memristor-based Chua's circuit: Dimensionality decreasing model for detecting extreme multistability," *IEEE Trans. Ind. Electron.*, vol. 67, no. 3, pp. 2197–2206, Mar. 2020.

[2] E. G. Nepomuceno, J. H. M. Rodrigues, S. A. M. Martins, P. Matjaž, and S. Mitja, "Interval computing periodic orbits of maps using a piecewise approach," *Appl. Math. Comput.*, vol. 336, pp. 67–75, Nov. 2018.

[3] E. G. Nepomuceno, A. M. Lima, J. Arias-García, M. Perc, and R. Repnik, "Minimal digital chaotic system," *Chaos Solitons Fractals*, vol. 120, pp. 62–66, Mar. 2019.

[4] K. Eshraghian *et al.*, "Memristive device fundamentals and modeling: Applications to circuits and systems simulation," *Proc. IEEE*, vol. 100, no. 6, pp. 1991–2007, Jun. 2012.

[5] F. Z. Wang, "A triangular periodic table of elementary circuit elements," *IEEE Trans. Circuits Syst. I, Reg. Papers*, vol. 60, no. 3, pp. 616–623, Mar. 2013.

[6] F. Corinto and M. Forti, "Memristor circuits: Bifurcations without parameters," *IEEE Trans. Circuits Syst. I, Reg. Papers*, vol. 64, no. 6, pp. 1540–1551, Jun. 2017.

[7] S. Chen, S. Yu, J. Lü, G. Chen, and J. He, "Design and FPGA-based realization of a chaotic secure video communication system," *IEEE Trans. Circuits Syst. Video Technol.*, vol. 28, no. 9, pp. 2359–2371, Sep. 2018.

[8] Z. Hua, Y. Zhou, and B. Bao, "Two-dimensional sine chaotification system with hardware implementation," *IEEE Trans. Ind. Informat.*, vol. 16, no. 2, pp. 887–897, Feb. 2020.

[9] B. Bao, H. Li, H. Wu, X. Zhang, and M. Chen, "Hyperchaos in a second-order discrete memristor-based map model," *Electron. Lett.*, vol. 56, no. 15, pp. 769–770, Jul. 2020.

[10] C. Li, B. Feng, S. Li, J. Kurths, and G. Chen, "Dynamic analysis of digital chaotic maps via state-mapping networks," *IEEE Trans. Circuits Syst. I, Reg. Papers*, vol. 66, no. 6, pp. 2322–2335, Jun. 2019.

[11] Z. Hua, Y. Zhou, C. M. Pun, and C. L. P. Chen, "2D Sine Logistic modulation map for image encryption," *Inf. Sci.*, vol. 297, pp. 80–94, Mar. 2015.

[12] H. Jiang, Y. Liu, Z. Wei, and L. Zhang, "Hidden chaotic attractors in a class of two-dimensional maps," *Nonlinear Dyn.*, vol. 85, no. 4, pp. 2719–2727, Sep. 2016.

[13] S. Panahi, J. Sprott, and S. Jafari, "Two simplest quadratic chaotic maps without equilibrium," *Int. J. Bifurcation Chaos*, vol. 28, no. 12, Dec. 2018, Art. no. 1850144.

[14] D. Abbasinezhad-Mood and M. Nikooghadam, "Efficient anonymous password-authenticated key exchange protocol to read isolated smart meters by utilization of extended Chebyshev chaotic maps," *IEEE Trans. Ind. Informat.*, vol. 14, no. 11, pp. 4815–4828, Nov. 2018.

[15] H. Li, Z. Hua, H. Bao, L. Zhu, M. Chen, and B. Bao, "Two-dimensional memristive hyperchaotic maps and application in secure communication," *IEEE Trans. Ind. Electron.*, early access, Sep. 15, 2020, doi: 10.1109/TIE.2020.3022539.

[16] B. Bao, Z. Liu, and J. Xu, "Steady periodic memristor oscillator with transient chaotic behaviours," *Electron. Lett.*, vol. 46, no. 3, pp. 228–230, Feb. 2010.

[17] R. M. May, "Simple mathematical models with very complicated dynamics," *Nature*, vol. 261, no. 5560, pp. 459–467, Jul. 1976.

[18] L. Chua, "If it's pinched it's a memristor," *Semicond. Sci. Technol.*, vol. 29, no. 10, Sep. 2014, Art. no. 104001.

[19] V. Landassuri-Moreno, J. R. Marcial-Romero, A. Montes-Venegas, and M. A. Ramos, "Chaotic time series prediction with feature selection evolution," in *Proc. IEEE Electron. Robot. Autom. Mech. Conf.*, 2011, pp. 71–76.

[20] R. Mikolajczak and J. Mandziuk, "Comparative study of logistic map series prediction using feed-forward, partially recurrent and general regression networks," in *Proc. 9th Int. Conf. Neural Inf. Process.*, 2002, pp. 2364–2368.

[21] H. Bao, Z. Hua, N. Wang, L. Zhu, M. Chen, and B. Bao, "Initials-boosted coexisting chaos in a 2D sine map and its hardware implementation," *IEEE Trans. Ind. Informat.*, vol. 17, no. 2, pp. 1132–1140, Feb. 2021.

[22] H. Bao, M. Chen, H. Wu, and B. Bao, "Memristor initial-boosted coexisting plane bifurcations and its extreme multi-stability reconstitution in two-memristor-based dynamical system," *Sci. China Technol. Sci.*, vol. 63, no. 4, pp. 603–613, Apr. 2020.

[23] C. Bandt and B. Pompe, "Permutation entropy: A natural complexity measure for time series," *Phys. Rev. Lett.*, vol. 88, no. 17, Apr. 2002, Art. no. 174102.

[24] J. Theiler, "Efficient algorithm for estimating the correlation dimension from a set of discrete points," *Phys. Rev. A*, vol. 36, no. 9, pp. 4456–4462, Nov. 1987.

[25] P. Jin, G. Wang, H. H.-C. Iu, and T. Fernando, "A locally active memristor and its application in a chaotic circuit," *IEEE Trans. Circuits Syst. II, Exp. Briefs*, vol. 65, no. 2, pp. 246–250, Feb. 2018.